Original Article

MOLECULAR METABOLISM

Maresin 1 activates brown adipose tissue and promotes browning of white adipose tissue in mice

Laura M. Laiglesia [1,2,17], Xavier Escoté [1,2,3,17], Neira Sáinz [1,2], Elisa Felix-Soriano [1,2], Eva Santamaría [4,5], María Collantes [6,7], Marta Fernández-Galilea [1,2,7], Ignacio Colón-Mesa [1,2], Leyre Martínez-Fernández [1,2], Tania Quesada-López [8,10], Sergio Quesada-Vázquez [3], Carlos Rodríguez-Ortigosa [5], José M. Arbones-Mainar [9,10], Ángela M. Valverde [11,12], J Alfredo Martínez [1,2,7,10], Jesmond Dalli [13,14], Laura Herrero [10,15], Silvia Lorente-Cebrián [1,2,7,16], Francesc Villarroya [8,10], María J. Moreno-Aliaga [1,2,7,10,*]

ABSTRACT

Objective: Maresin 1 (MaR1) is a docosahexaenoic acid-derived proresolving lipid mediator with insulin-sensitizing and anti-steatosis properties. Here, we aim to unravel MaR1 actions on brown adipose tissue (BAT) activation and white adipose tissue (WAT) browning.

Methods: MaR1 actions were tested in cultured murine brown adipocytes and in human mesenchymal stem cells (hMSC)-derived adipocytes. *In vivo* effects of MaR1 were tested in diet-induced obese (DIO) mice and lean WT and *Il6* knockout ($Il6^{-/-}$) mice.

Results: In cultured differentiated murine brown adipocytes, MaR1 reduces the expression of inflammatory genes, while stimulates glucose uptake, fatty acid utilization and oxygen consumption rate, along with the upregulation of mitochondrial mass and genes involved in mitochondrial biogenesis and function and the thermogenic program. In Leucine Rich Repeat Containing G Protein-Coupled Receptor 6 (LGR6)-depleted brown adipocytes using siRNA, the stimulatory effect of MaR1 on thermogenic genes was abrogated. In DIO mice, MaR1 promotes BAT remodeling, characterized by higher expression of genes encoding for master regulators of mitochondrial biogenesis and function and iBAT thermogenic activation, together with increased M2 macrophage markers. In addition, MaR1-treated DIO mice exhibit a better response to cold-induced BAT activation. Moreover, MaR1 induces a beige adipocyte signature in inguinal WAT of DIO mice and in hMSC-derived adipocytes. MaR1 potentiates *Il6* expression in brown adipocytes and BAT of cold exposed lean WT mice. Interestingly, the thermogenic properties of MaR1 were abrogated in $Il6^{-/-}$ mice.

Conclusions: These data reveal MaR1 as a novel agent that promotes BAT activation and WAT browning by regulating thermogenic program in adipocytes and M2 polarization of macrophages. Moreover, our data suggest that LGR6 receptor is mediating MaR1 actions on brown adipocytes, and that IL-6 is required for the thermogenic effects of MaR1.

Keywords Maresin 1; Obesity; Brown/beige adipose tissue; Interleukin-6; LGR6

[1]University of Navarra, Center for Nutrition Research, Pamplona, 31008, Spain [2]University of Navarra, Department of Nutrition, Food Science and Physiology, Pamplona, 31008, Spain [3]Eurecat, Centre Tecnològic de Catalunya, Unitat de Nutrició i Salut, Reus, 43204 Spain [4]Centro de Investigación Biomédica en Red de Enfermedades Hepáticas y Digestivas (CIBEREHD), Instituto de Salud Carlos III (ISCIII), Madrid 28029, Spain [5]Division of Hepatology, Center for Applied Medical Research, University of Navarra, Pamplona, Spain [6]Department of Nuclear Medicine/ Translational Molecular Imaging Unit (UNIMTRA), Clínica Universidad de Navarra, Pamplona, 31008, Spain [7]Navarra Institute for Health Research (IdiSNA), Pamplona, Spain [8]Department of Biochemistry and Molecular Biomedicine, Institute of Biomedicine of the University of Barcelona, Barcelona, Catalonia, Spain [9]Adipocyte and Fat Biology Laboratory (AdipoFat), Instituto de Investigación Sanitaria Aragón, Instituto Aragonés de Ciencias de la Salud, Unidad de Investigación Traslacional, Hospital Universitario Miguel Servet, Zaragoza, Spain [10]Centro de Investigación Biomédica en Red de Fisiopatología de la Obesidad y Nutrición (CIBEROBN), Instituto de Salud Carlos III (ISCIII), Madrid, Spain [11]Alberto Sols Biomedical Research Institute (IIBm) (CSIC/UAM), Madrid, Spain [12]Centro de Investigación Biomédica en Red de Diabetes y Enfermedades Metabólicas Asociadas (CIBERDEM), Instituto de Salud Carlos III (ISCIII), Madrid, Spain [13]William Harvey Research Institute, Barts and the London School of Medicine and Dentistry, Queen Mary University of London, London, UK [14]Center for Inflammation and Therapeutic Innovation, Queen Mary University of London, London, UK [15]Department of Biochemistry and Physiology, School of Pharmacy and Food Sciences, Institut de Biomedicina de la Universitat de Barcelona (IBUB), Universitat de Barcelona, Barcelona, Spain [16]Current address: Department of Pharmacology, Physiology, Legal and Forensic Medicine. Faculty of Health and Sport Science, University of Zaragoza, Zaragoza, Spain

[17] Equal authorship.

*Corresponding author. Center for Nutrition Research and Dept. Nutrition, Food Science and Physiology. School of Pharmacy and Nutrition. University of Navarra. C/. Irunlarrea, 1. 31008 Pamplona, Spain. E-mail: mjmoreno@unav.es (M.J. Moreno-Aliaga).

Received May 22, 2022 • Revision received May 19, 2023 • Accepted June 1, 2023 • Available online 2 June 2023

https://doi.org/10.1016/j.molmet.2023.101749

1. INTRODUCTION

Brown adipose tissue (BAT) activation has been brought to attention, since it provides a protective mechanism against excessive body weight and fat mass accumulation [1]. Beyond thermogenesis, emerging roles of BAT activation have been described, including control of triglyceride clearance [2], glucose homeostasis and insulin sensitivity [3–5] and, recently, BAT has been identified as an endocrine tissue [6]. In white adipose tissue (WAT), beige adipocytes can also dissipate energy as heat [7], and white-to-beige conversion has been pointed out as a potential therapy against obesity and insulin resistance [8]. BAT activation and WAT browning occur in response to certain stimuli such as β3-adrenergic stimulation and chronic cold exposure [9]. However, associated side effects and uncomfortableness respectively, limit their therapeutic applications. Consequently, the identification of new therapeutic agents capable of activating BAT and promoting WAT browning in an attempt to ameliorate obesity-associated metabolic disorders is highly encouraged.

A variety of bioactive lipid metabolites derived from polyunsaturated fatty acids (PUFAs), like Prostacyclin (PGI2), Prostaglandin E2 (PGE2), Prostaglandin F2alpha (PGF2α) and 12,13-DiHOME have been identified as novel regulators of thermogenesis in BAT and beige adipocytes [10–12]. Particularly, n-3 PUFAs have been described as inducers of BAT activity and WAT browning in mice [13]. The n-3 PUFAs eicosapentaenoic acid (EPA) and docosahexaenoic acid (DHA) are substrates for the formation of specialized proresolving lipid mediators (SPMs), including resolvins, protectins and maresins that actively participate in the resolution of inflammation in several tissues including WAT [14]. Maresin 1 (MaR1) is a DHA-derived SPM that was first identified in macrophages and more recently in other tissues [15,16]. MaR1 and its precursor promote the shift of macrophage phenotype toward an M2 profile [17]. Recently, we and others found that MaR1 modulates adipokine secretion in human white adipocytes and attenuates WAT inflammation, improves insulin sensitivity, and reduces liver steatosis in animal models of obesity [16,18–22]. It has been described that 12-lipoxygenase (12-LOX), an enzyme involved in the biosynthesis of MaR1, regulates cold adaptation in brown fat [23]. A recent lipidomic study carried out by our group detected MaR1 in BAT of mice and found that MaR1 levels are negatively correlated with the expression of *C–C motif chemokine ligand 2* (*Ccl2*), a proinflammatory gene [24]. However, whether MaR1 can activate BAT and/or promote WAT browning remains elusive.

In the present study, we found that MaR1 promotes thermogenic activation of brown murine adipocytes and induces browning of cultured human mesenchymal stem cells (hMSC)-derived adipocytes. MaR1 is also an activator of interscapular BAT (iBAT) and induces browning of inguinal WAT (iWAT) *in vivo* in diet-induced obese (DIO) mice. Using interleukin-6 (*Il6*) knockout ($Il6^{-/-}$) mice, we also demonstrated that IL-6 is required for MaR1 stimulatory actions on iBAT activation and iWAT browning under cold exposure. Moreover, studies using siRNA-mediated Leucine Rich Repeat Containing G Protein-Coupled Receptor 6 (LGR6) knock-down suggest that this receptor is mediating MaR1 actions in brown mature adipocytes.

2. MATERIALS AND METHODS

2.1. Mice models and treatments

All experimental procedures were performed under protocols approved by the University of Navarra Ethics Committee and Animal Ethics Committee of Eurecat for the use of laboratory animals, according to the National and Institutional Guidelines for Animal Care and Use (Protocols number: 047-15; E59-16(047-15E1); 090c-17; 110-17; 032-20; 10281).

2.1.1. Chronic MaR1 treatment to diet-induced obese mice

C57BL/6J male mice (7 weeks old) were obtained from Harlan Laboratories (Barcelona, Spain), and housed in plastic cages (three-four animals *per* cage) under controlled conditions (22 ± 2 °C, 12 h light–dark cycle, relative humidity, 55 ± 10%). Animals were fed a standard mouse pelleted chow diet (13% of kcal from fat, 67% from carbohydrates and 20% from protein) from Harlan Teklad Global Diets (Harlan Laboratories, Indianapolis, IN, USA) for an adaptation period of 7 days. Then, one group (Control) was fed *ad libitum* with standard mouse chow (control) diet, and a second group (DIO) with a high-fat diet (60% of kcal from fat, 20% from carbohydrates and 20% from protein) provided by ResearchDiets (New Brunswick, USA) for three months. Thereafter, the control group received a daily oral gavage of the vehicle (100 μl of sterile saline-0.1% ethanol) for 10 days. Additionally, DIO mice were assigned into two subgroups that received a daily oral gavage of the vehicle or MaR1 (50 μg/kg body weight, Cayman, Ann Arbor, MI, USA) for 10 days.

2.1.2. Acute MaR1 treatment to wild type and Il6 knock-out mice

$Il6^{-/-}$ mice were a generous gift from the group of Prof. Ávila (University of Navarra) and were housed as described above. WT (C57BL/6J) and $Il6^{-/-}$ male animals (8 weeks old) were fed control diet. After a single injection with MaR1 (50 μg/kg; i. p.) or vehicle, animals were housed at 4 °C for 24 h. Body weight and rectal temperature (Thermometer pb 0331, Panlab, Barcelona, Spain) were measured before and after treatment.

2.1.3. *In vivo* study of iBAT activation by positron emission tomography (PET)

BAT activation after both acute and chronic treatment with MaR1 was studied *in vivo* by PET with the radiotracer ^{18}F-fluorodeoxyglucose (^{18}F-FDG). In the chronic treatment, MaR1 (50 μg/kg; 10 days, oral gavage) or vehicle were administered to DIO mice as described above. In the acute treatment, MaR1 (50 μg/kg; i. p.) or vehicle were injected to male lean WT and $Il6^{-/-}$mice. Thirty minutes after administration, iBAT was stimulated by cold exposure during 1 h at 4 °C [25]. After cold exposure, ^{18}F-FDG (10.1 ± 0.9 MBq) was injected through the tail vein. PET static images were acquired 1 h (room temperature) post ^{18}F-FDG injection in a small animal PET scanner (Mosaic, Philips, Amsterdam, Netherlands). For each study, animals were anesthetized with 2% isoflurane in 100% O_2 gas. All studies were analyzed using PMOD software (PMOD Technologies Ltd., Adliswil, Switzerland). For semiquantitative analysis, ^{18}F-FDG uptake by BAT was evaluated drawing volume-of-interest (VOIs) on coronal PET images including the interscapular BAT (iBAT). From each VOI, maximum standardized uptake value (SUVmax) was calculated using the formula SUV = [tissue activity concentration (Bq/cm^3)/injected dose (Bq)] × body weight (g).

2.1.4. Thermography imaging

In vivo BAT area temperature of mice was measured as previously described [26]. Briefly, temperature of the skin BAT area was measured by infrared thermal images after 1 h cold exposure (4 °C) with or without MaR1 (50 μg/kg, i. p.) in lean WT and $Il6^{-/-}$ mice. Temperatures were recorded using a T335 infrared digital thermal imaging camera (FLIR Systems, Wilsonville, OR, USA), which features a thermal sensitivity of 0.1 °C. Environmental parameters (relative humidity, room temperature and reflected apparent temperature) were

measured *in situ* and set in the camera as parametric inputs from the experiment. Triplicate infrared pictures of non-anaesthetized animals were taken from 30 cm. Mice were shaved 48 h before thermographic measurements. The resulting images were analysed using the FLIR QuickReport 1.2 software (FLIR Systems). Maximal temperature values from the BAT area were retrieved.

2.1.5. Whole body indirect calorimetry

Whole-body indirect calorimetry analyses were performed using the OxyletProTM System (Panlab, Cornellà, Spain) in seven C57BL/6J male (8-weeks-old) mice treated intraperitoneally with vehicle, and after a week of washout, treated with MaR1 (50 μg/kg). Just after receiving vehicle or MaR1 treatments (at 10 am), mice were transferred to an acrylic box (Oxylet LE 1305 Physiocage, Panlab) with free access to water and food. After 1 h of acclimation period, oxygen consumption (VO_2) and carbon dioxide production (VCO_2) were measured every 15 min by an O_2 and CO_2 analyzer (Oxylet LE 405 gas analyzer, Panlab) at a constant flow rate of 600 mL/min (Oxylet LE 400 air supplier, Panlab). At each measure, the program Metabolism 2.1.02 (Panlab) calculated the respiratory quotient (RER) as the VCO_2/VO_2 ratio and energy expenditure (EE) as $VO_2 \times 1.44 \times [3.815 + (1.232 \times RER)]$ (kcal/day/kg0.75) [27].

2.2. Cellular and tissue models

2.2.1. Brown adipocytes culture and treatments

Primary brown adipocytes were obtained from the iBAT of neonatal mice and immortalized as previously described [28]. Brown pre-adipocytes were differentiated as described [29]. Briefly, immortalized brown pre-adipocytes were grown in high glucose DMEM (Gibco™) supplemented with 10% fetal bovine serum (FBS; Gibco™), 20 nM insulin (Sigma–Aldrich) and 2 nM triiodothyronine (T3; Sigma–Aldrich) (differentiation medium, DM) until reaching confluence. Next, the cells were cultured for 2 days in induction medium (IM) consisting of DM supplemented with 0.5 μM dexamethasone (Sigma–Aldrich), 0.125 μM indomethacin (Sigma–Aldrich), 1 μM rosiglitazone (Sigma–Aldrich) and 0.5 mM isobutyl-methyl-xanthine (IBMX; (Sigma–Aldrich). Then, cells were cultured in DM until day 7 in which they exhibited a fully differentiated phenotype. Brown mature (fully differentiated) adipocytes were treated with vehicle or MaR1 (0.1 and 1 nM for 24 h). In other set of experiments, brown adipocytes were treated with other SPMs such as Maresin 2 (MaR2), Resolvin D1 (RvD1) and Resolvin D2 (RvD2), at concentrations of 0.1 and 1 nM for 24 h.

Changes in the temperature of brown cultured adipocytes were measured as previously described [13]. Brown adipocytes were grown in a 12-well plate and placed on a 37 °C heat block in a polystyrene box coated with black paper to optimize insulation. Images were acquired and analyzed with the same infrared camera and software pointed above for mice.

2.2.2. Culture and differentiation of brown preadipocytes from iBAT of WT and Fgf21$^{-/-}$ mice

Stromal vascular cells were obtained from iBAT excised from WT and their counterparts *Fgf21* knockout mice (*Fgf21*$^{-/-}$) (3 weeks old; males and females) in Dr. Villarroya's laboratory (UB, Barcelona, Spain). Primary cultures were induced to differentiate into brown adipocytes, following the previously reported procedures [13]. Briefly, brown adipocyte differentiation was achieved by exposing confluent precursor cells from iBAT in DMEM/F12 medium containing 10% FBS and supplemented with 20 nM insulin, 2 nM T3, and 0.1 mM ascorbic acid. Then, mature brown adipocytes were treated with vehicle or MaR1 (1 nM, 24 h).

2.2.3. iBAT and iWAT explants

WT and *Il6*$^{-/-}$ mice (8 weeks old) were sacrificed and iBAT and iWAT were removed, washed with PBS and chopped into 8 parts small 1 mm^2 pieces to generate fat explants that were seed for 2 h in high glucose DMEM (Gibco™) containing 2% bovine serum albumin (BSA; Sigma–Aldrich) [30,31]. After 30 min of acclimation, explants were treated with vehicle or MaR1 (1 nM; 3 h) at 37 °C. Then explants were harvested and stored for protein or mRNA extraction.

2.2.4. Human mesenchymal stem cells (hMSC) culture and treatments

hMSC from subcutaneous abdominal adipose tissue of non-diabetic obese male and female subjects (BMI: 30–41 kg/m^2) undergoing elective laparoscopic surgery were obtained by Dr. Arbones-Mainar (Instituto Aragonés de Ciencias de la Salud, Zaragoza, Spain). This study was approved by the Institutional Review Board (Research Ethic Committee of Aragón, CEICA 20/2014), and informed consent was obtained from all participants. hMSC were isolated and maintained as previously described [19,32]. To study the effects of MaR1 treatment during the differentiation process, MaR1 (1, 10 and 100 nM) was added on confluent un-differentiated hMSC cells at the same time of the adipogenic cocktail and then added to fresh medium ever after.

2.2.5. RAW 264.7 macrophages culture and treatments

RAW 264.7 cells (murine macrophage cell line) were grown in complete medium Roswell Park Memorial Institute (RPMI; Gibco™ 1640) supplemented with 10% FBS, 50 U/mL penicillin, and 50 μg/U/mL streptomycin (Gibco™). Cells were untreated or stimulated with bacterial lipopolysaccharide (LPS; Invitrogen) at 100 ng/mL for 24 h and with vehicle or MaR1 (0.1, 1 nM; 24 h). Then, macrophages were collected for analysis of extracted RNA and culture media were collected and centrifuged at 1,950 *g* for 20 min, and filtered through 0.22 μm filters (Millipore, Billerica, MA, USA) to remove cells and debris. Control medium or conditioned media of RAW macrophages (25%) were used to treat mature brown adipocytes for 24 h with vehicle or MaR1 (0.1, 1 nM; 24 h).

2.3. Biochemical analyses

Serum insulin levels of mice were determined by ELISA (Mercodia, Uppsala, Sweden) according to the manufacturer's guidelines. Fasting glucose levels were measured with a standard glucometer (Accu-Check Advantage blood glucose meter, Roche, Basel, Switzerland). Levels of of fibroblast growth factor (FGF21) in brown adipocytes culture medium and IL-6 levels in serum were measured by Milliplex ELISA kit (Merck, Madrid, Spain).

2.4. Body composition

Body composition was measured in mice before and at the end of the study by QMR technology (EchoMRI-100-700, Echo Medical Systems, Houston, TX, USA) as previously described [19].

2.5. Histological analysis of iBAT and iWAT

iBAT and iWAT pieces of DIO mice treated with vehicle or MaR1 (50 μg/kg; oral gavage for 10 days) were fixed in 4.3% neutral formalin (pH 7.4) for 24 h, dehydrated with 70% ethanol, and embedded in paraffin. Five μm thick sections were deparaffinized and stained with haematoxylin-eosin (H&E) or treated for immunofluorescence (IHF) studies. iBAT and iWAT images (magnification 100×) were taken with the camera Nikon SMZ18 (Nikon Instruments Europe, Amsterdam, Netherlands). Mean lipid droplet area in adipose tissue H&E-stained samples was quantified with ImageJ 2.0 imaging suite (U.S. National

Institutes of Health, Bethesda, MD, USA). For IHF, rehydrated tissue sections were blocked with 3% BSA for 1 h at room temperature. Preparations were then incubated with CD206 (Proteintech, Rosemont, IL, USA) antibody followed by IgG secondary antibody (Alexa fluor 488 Goat anti-Rabbit). Immunofluorescence signals were visualized under a fluorescence microscope ZOE Fluorescent Cell Imager, Bio-Rad, Hercules, CA, USA) and quantified using the ImageJ 2.0 imaging suite.

2.6. 2-Deoxy-D-glucose (2-DG) uptake in brown adipocytes

2-DG uptake was measured as previously described [33]. Briefly, fully differentiated mature brown adipocytes treated with vehicle or MaR1 (0.1–1 nM; 24 h), followed a 2-h period of glucose deprivation. Then, cells were incubated with 0.1 μL/mL of 2-DG (Sigma–Aldrich, St. Louis, CA, USA) and 0.2 μCi/mL of ^{14}C-2-DG (Deoxy-D-glucose, 2-[1–^{14}C], American Radiolabeled Chemicals) for 15 min. Then, cell lysates were taken to measure ^{14}C-2-DG radioactivity by liquid scintillation counting, HIDEX 300 SL scintillation counter (Hidex Oy, Turku, Finland). Results were normalized to total protein content of cell extracts.

2.7. Fatty acid oxidation determination in brown adipocytes

Fatty acid oxidation was determined by the sum of $^{14}CO_2$ liberated to the media and ^{14}C-acid soluble metabolites (ASM) as previously described [34]. For that purpose, fully differentiated mature brown adipocytes were treated with vehicle or MaR1 (0.1–1 nM; 24 h). Briefly, differentiated brown adipocytes were incubated for 4 h in Krebs–Ringer buffer without glucose, containing 125 mM NaCl, 5 mM KCl, 2 mM $CaCl_2$, 1.25 mM KH_2PO_4, 1.25 mM $MgSO_4 \cdot 7H_2O$, 25 mM $NaHCO_3$ and 3% fatty acid-free bovine serum albumin (BSA) pH 7.8, 2 mM L-carnitine, 80 μM palmitic acid (Sigma), and 20 μM ^{14}C-palmitic acid (58 μCi/μmol, Perkin Elmer; Waltham, MA). The medium was transferred to a glass vial with a central well containing benzethonium hydroxide (Sigma).

$^{14}CO_2$ was liberated by acidification with 1 M H_2SO_4 and collected during 2 h in the central well. $^{14}CO_2$ was measured by scintillation counting in a scintillation counter HIDEX 300 SL (Hidex Oy, Turku, Finland). Cells were washed and then scraped in cold buffer (0.25 M sucrose; 10 mM Tris–HCl; 1 mM EDTA; 1 mM dithiothreitol, pH 7.4). Neutral lipids and ASM were separated by adding 5 vol chloroform/methanol (2:1) and 0.4 vol 1 M KCl/HCl. Specific activity was measured and used to calculate total oxidation as equivalent of oxidized palmitic acid. Results were normalized to total protein content of cell extracts.

2.8. Free fatty acids uptake in brown adipocytes

Fully differentiated mature brown adipocytes were treated with vehicle or MaR1 (0.1–1 nM; 24 h) and free fatty acids uptake (^{14}C 2-Bromopalmitate incorporation, Moraveck Biochemicals, Brea, CA, USA) was measured as previously described [34]. Adipocytes were incubated in Krebs–Ringer buffer during 50 min and after this period of time, cold palmitic acid, carnitine and the non-metabolizable analogue 2-Bromopalmitic acid (Moraveck Biochemicals, Brea, CA) were added to the media in a final concentration of 2 mM L-carnitine, 80 μM palmitic acid (Sigma), and 20 μM ^{14}C-2-Bromopalmitic acid and incubated for 10 min. Culture plates were then put on ice and rinsed twice with cold PBS. Cells were scraped in 0.05 M NaOH, and ^{14}C-2-Bromopalmitic acid uptake was measured by liquid scintillation counting of cell lysates. The results were normalized to the total protein content of cell lysates.

2.9. Analysis of adipocyte oxygen consumption in brown adipocytes

Oxygen Consumption Rate (OCR) was measured in mature brown adipocytes (treated with vehicle or MaR1 0.1 nM; 24 h) using Seahorse Extracellular Flux (XF) 24 Analyser (Agilent Technologies, Santa Clara, CA, USA). Briefly, 1 h prior the assay, the adipocytes were washed thoroughly with assay medium (DMEM supplemented with 50 mM glucose and 1 mM sodium pyruvate) and incubated in a CO_2-free incubator at 37 °C. During the assay, oligomycin (1 μg/mL), carbonylcyanide-4-(trifluoromethoxy) phenylhydrazone (FCCP; 0.6 μM), and a mixture of rotenone and antimycin A (2 μM of each one), were sequentially injected for OCR measurement to obtain the values for the basal mitochondrial respiration, ATP-linked, proton leak, maximal respiratory capacity, reserve capacity and non-mitochondrial respiration. The results were normalized to total protein content.

2.10. Mitotracker staining in brown adipocytes

MitoTracker green FM stainings were performed as described by the manufacturer (M7514; Molecular Probes, Invitrogen). Briefly, fully differentiated mature brown adipocytes, treated with vehicle or MaR1 (0.1, 1 nM; 24h) were incubated with 100 nM MitoTracker® Green FM for 30 min at 37 °C in serum free medium. Then, brown adipocytes were washed with PBS prior to imaging with the fluorescence microscope ZOE Fluorescent Cell Imager (Bio-Rad, Hercules, CA, USA). Fluorescence signal of MitoTracker® Green FM probe was quantified using the Fluoroskan Ascent FL Fluorometer (Thermo Fisher Scientific) (485 nm excitation and 538 nm emission).

2.11. siRNA transfection in brown adipocytes

Brown adipocytes were transfected with siRNA at day 5 of differentiation as follows: negative control siRNA, *Lgr6* siRNA and Lipofectamine RNAiMAX (Life Technologies, 13778-100) were diluted in Opti-MEM I Reduced Serum Medium (Life Technologies, 31985-062) separately before being mixed by pipetting and left to incubate for 5 min at room temperature. Then, the siRNA-RNAiMAX mix was added drop to drop to brown adipocytes in high glucose DMEM supplemented with 10% FBS (Gibco™), 20 nM insulin (Sigma–Aldrich), 2 nM T3 (Sigma–Aldrich), without penicillin and streptomycin and left to incubate for 24 h. The final concentrations of Lipofectamine RNAiMAX and siRNA were 5 μL/mL and 50 nM, respectively. One day after transfection, brown adipocytes were treated with vehicle or MaR1 (0.1, 1 nM; 24h) and supernatants and cells were collected.

2.12. Targeted lipidomics

Targeted lipidomic assays of Maresins biosynthesis pathway was carried out as previously described [24]. All samples were extracted using solid-phase extraction columns as previously described [35,36]. Prior to sample extraction, deuterated internal standards, representing each region in the chromatographic analysis (500 pg each) were added to facilitate quantification in 1 mL of methanol. Samples were kept at −20 °C for a minimum of 45 min to allow protein precipitation. Supernatants were subjected to solid-phase extraction, methyl formate and methanol fractions were collected, brought to dryness, and suspended in phase (methanol/water, 1:1, vol/vol) for injection on a Shimadzu LC-20CE HPLC and a Shimadzu SIL-20AC autoinjector (Shimadzu Corp., Kyoto, Japan), paired with a QTrap 6500+ (Sciex, Warrington, UK). For identification and quantitation of products eluted in the methyl formate an Agilent Poroshell 120 EC-C18 column (100 mm × 4.6 mm × 2.7 μm, Agilent Technologies, Santa. Clara, CA, USA) was kept at 50 °C and mediators eluted using a mobile phase consisting of methanol–water-acetic acid of 20:80:0.01 (vol/vol/vol) that was ramped to 50:50:0.01 (vol/vol/vol) over 0.5 min at flow rate of 0.5 mL/min. The gradient was then ramped to 80:20:0.01 (vol/vol/vol) from 2 min to 11 min, maintained till 14.5 min at a flow rate of 0.35 mL/min, and then, rapidly ramped to 98:2:0.01 (vol/vol/vol) for.

the next 0.1 min. This was subsequently maintained at 98:2:0.01 (vol/vol/vol) for 5.4 min, and the flow rate was maintained at 0.5 mL/min. QTrap 6500+ was operated using a multiple reaction monitoring method coupled with information-dependent acquisition and enhanced production scan. Each LM was identified using established criteria, including 1) matching retention time to synthetic and authentic materials, 2) the integrated peak consists of at least 7 data points, and 3) the signal-to-noise ratio of the integrated peak is at least 5. Calibration curves were obtained for each using synthetic compound mixtures at 0.78, 1.56, 3.12, 6.25, 12.5, 25, 50, 100, and 200 pg that gave linear calibration curves with an r^2 values of 0.98−0.99 [37].

2.13. Analysis of protein levels by Western blot

iWAT and iBAT lysates of mice were obtained as previously described [19]. Membranes were probed with specific primary antibodies against uncoupling protein 1 (UCP1) (1:1,000; Abcam, Cambridge, UK) and β-Actin (1:5,000; Sigma−Aldrich). Thereafter, infrared fluorescent secondary antibodies anti-rabbit (1:15,000; Cell Signaling Technology, Danvers, MA, USA) and anti-mouse (1:15,000; LI-COR Biosciences, Lincoln, NE USA) were used and quantitated using an Odyssey® infrared imaging system (LI-COR).

2.14. Analysis of mRNA levels

Total RNA was isolated from fully differentiated brown adipocytes and hMSC-derived adipocytes, as well as from iWAT and iBAT of mice, and then reverse transcribed to cDNA as previously described [34]. mRNA levels were determined using predesigned Taqman® Assays-on-Demand (Applied Biosystems, Waltham, MA, USA) or analyzed by Power SYBR Green PCR Master Mix (Bio-Rad) using the Touch Real-Time PCR System (CFX384, Bio-Rad). *Cyclophilin A (Ppia)*, *36B4* and *18S* were used as housekeeping genes (see Tables S1 and S2 for primers information). Relative expression of the genes was calculated by the $2^{-\Delta\Delta Ct}$ method [38].

2.15. Statistical analysis

GraphPad Prism 9 software (Graph-Pad Software Inc., San Diego, CA, USA) was used for statistical analyses and significant ($p < 0.05$) differences between groups were reported. Data are presented as mean ± SEM. Comparisons between the values for different variables were analyzed by one-way ANOVA followed by Bonferroni *post hoc* tests or by Student's *t*-tests or Mann−Whitney U-tests once the normality had been screened using Kolmogorov−Smirnov and Shapiro−Wilk tests.

3. RESULTS AND DISCUSSION

3.1. Maresin 1 promotes glucose uptake, fatty acid utilization, mitochondrial biogenesis, thermogenic gene expression and oxygen consumption in differentiated murine brown adipocytes

MaR1-treated murine brown adipocytes exhibited a significant upregulation of thermogenic genes (*Ucp1* and *Iodothyronine deiodinase 2, Dio2*), as well as genes related to glucose transport (*Solute carrier family 2 member 4*, *Glut4*) and fatty acid oxidation (*Carnitine palmitoyltransferase A*, *Cpt1a* and *Acyl-coenzyme A oxidase, Acox1*), while no significant changes were found in *Peroxisome proliferator-activated receptor alpha* (*Ppara*). MaR1 also upregulated the expression of genes involved in mitochondrial biogenesis (*Peroxisome proliferator-activated receptor gamma coactivator 1-alpha, Pgc1a; Mitochondrial transcription factor A, Tfam; Nuclear respiratory factor 1, Nrf1*), and function, such as *mitofusin 2* (*Mfn2*), an outer mitochondrial membrane GTPase critical for mitochondrial fusion and dynamics, that plays also a critical role in BAT thermogenesis [39,40] (Figure 1A). We also estimated mitochondrial content by using mitotracker green probes, which stain the mitochondrial matrix proteins independently of the mitochondrial membrane potential and, therefore, reflects mitochondrial mass [34]. Our data revealed an increase in mitochondrial mass in MaR1-treated brown adipocytes (Figure 1B). In parallel, basal oxygen consumption rate (OCR), maximal respiratory capacity and proton leak were significantly higher in brown adipocytes treated for 24 h with MaR1 (Figure 1C). Moreover, highly sensitive thermography [13] showed that MaR1 treatment increased the temperature of cultured brown adipocytes (Figure 1D). BAT activation requires fuel supply, which includes glucose and fatty acids [5,41]. Remarkably, MaR1 induced both fatty acid uptake and fatty acid oxidation (Figure 1E). Moreover, MaR1-treated brown adipocytes presented higher glucose uptake than controls (Figure 1F).

It has been shown that thermogenic activation of BAT induces the expression and release of FGF21 [42]. Moreover, the lipid sensor G-protein coupled receptor 120 (GPR120) plays a key role in BAT activation through the induction of FGF21 [13]. Here, we demonstrate that MaR1 treatment also upregulated *Gpr120* and *Fgf21* gene expression (Figure 1A), as well as induced FGF21 secretion (Figure 1G) in cultured murine brown adipocytes. To characterize whether FGF21 is involved in MaR1 actions on thermogenic genes, we tested MaR1 effects in differentiated primary brown adipocytes from preadipocytes obtained from the stroma-vascular fraction of iBAT of *Fgf21*-null mice. Figure 1H shows that the stimulatory effects of MaR1 on *Ucp1*, *Gpr120* and *PR domain containing 16* (*Prdm16*) were also observed and even increased in *Fgf21* deficient mice, suggesting that the increase in the production of FGF21 by brown adipocytes is not required for the thermogenic effects of this SPM. Surprisingly, the stimulatory actions of MaR1 on these genes were significantly higher in *Fgf21* knockout mice, suggesting that FGF21 could be interfering with some of the pathways mediating MaR1-actions in brown adipocytes. Notably, these MaR1 actions in brown adipocytes were observed using physiological doses (0.1−1 nM). In this regard, a recent study of our group found that MaR1 concentration in BAT of young (2-month-old) female mice at room temperature is around 0.15 pg/g tissue [24], which corresponds to 0.375 nM [16].

3.2. *In vivo* administration of MaR1 promotes iBAT activation and induces beige adipocyte markers in iWAT of DIO mice

We next examined whether *in vivo* administration of MaR1 (50 μg/kg, oral gavage, 10 days) was able to induce BAT activation in DIO mice. The histological examination of BAT revealed that MaR1-treated DIO mice exhibited smaller lipid droplets as compared to DIO-untreated mice and almost recovered the typical morphological features of iBAT observed in control fed animals (Figure 2A). Interestingly, MaR1-treated DIO mice displayed a significant increase on UCP1 protein levels (Figure 2B). Moreover, MaR1 reversed the downregulation of *Pgc1a* and *Prdm16* mRNA levels observed in iBAT of DIO mice, and upregulated the expression of *Sirtuin 1* (*Sirt1*), *Dio2*, *Gpr120, Fgf21* and *Mfn2* (Figure 2C). In parallel, MaR1 increased the expression of genes related to lipolysis (*Adipose triglyceride lipase*, *Atgl*), fatty acid oxidation (*Acox1*) and glucose uptake (*Glut1*, *Glut4*) (Figure 2D). In obesogenic conditions, iBAT is infiltrated by pro-inflammatory M1 macrophages, which can alter its ability to properly respond to thermogenic stimuli [43,44]. A study of our group revealed that MaR1 reduces macrophage infiltration in visceral WAT of DIO mice [19]. Here, we report that MaR1 treatment reversed the high fat diet-induced upregulation of *Ccl2, Tumor necrosis factor alpha (Tnfa)* and the proinflammatory M1 macrophage marker *CD11 Antigen-Like Family*

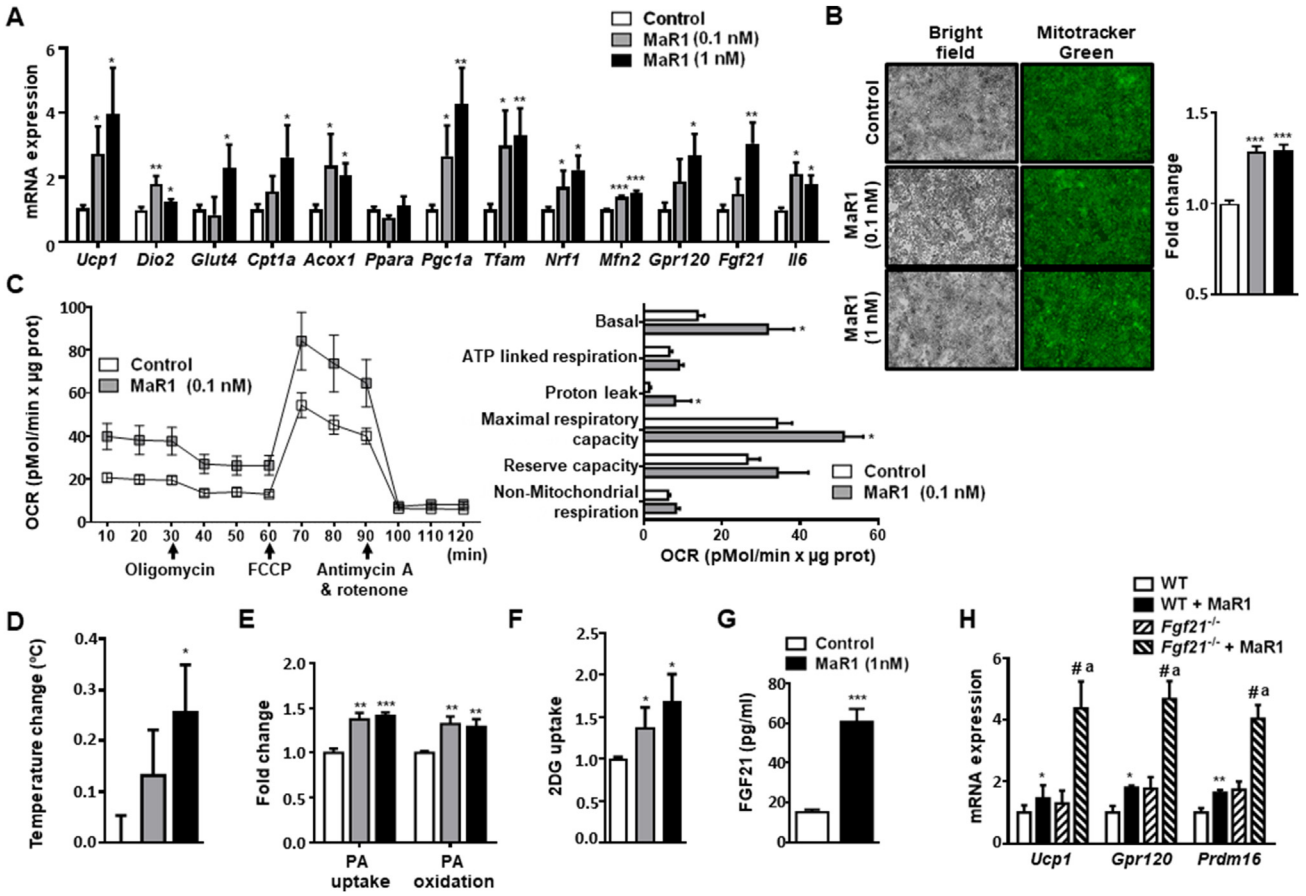

Figure 1: MaR1 upregulates thermogenic genes and promotes glucose uptake and fatty acid utilization in cultured fully differentiated murine brown adipocytes. (A) mRNA expression levels of genes involved in metabolism and function in murine brown adipocytes treated with MaR1 (0.1, 1 nM) for 24 h (n = 3–12). (B) Analysis of mitochondrial content by mitotracker green staining. Representative images and fluorescence intensity quantification of live cell imaging of mitochondria stained with mitotracker green FM probe (100 nM, 30 min) in murine brown adipocytes treated with MaR1 (0.1, 1 nM) for 24 h (n = 6). (C) Oxygen consumption rate (OCR) was measured in brown adipocytes (control and treated with MaR1 for 24 h) with a Seahorse technology. Left panel shows a representative experiment. Right panel: Bioenergetic parameters were inferred from the OCR traces. FCCP (carbonyl cyanide-p-trifluoromethoxyphenyl-hydrazon) (n = 3–4). (D) Changes in brown adipocytes temperature measured by highly sensitive thermography in mature brown adipocytes treated with vehicle or MaR1 (0.1, 1 nM) for 24 h (n = 8). (E–F) Palmitic acid (PA) uptake (^{14}C 2-Bromopalmitate incorporation) and Palmitate (PA) oxidation rates (E) and 2-Deoxy-D-glucose (2DG) uptake (F) in MaR1-treated brown adipocytes (n = 6–17). (G) FGF21 secretion levels in cultured media of brown adipocytes treated with vehicle or MaR1 (1 nM, 24 h) (n = 4). (H) Expression of thermogenic genes in differentiated brown adipocytes from wild type (WT) and *Fgf21*$^{-/-}$ mice treated with vehicle or MaR1 (1 nM, 24 h) (n = 3–4). Data are mean ± SEM (n = 3–17). mRNA expression, PA uptake and oxidation, and 2DG uptake data are expressed as fold change relative to control or WT cells-treated with vehicle and considered as 1. *p < 0.05; **p < 0.01; ***p < 0.001 *vs.* Control or WT (vehicle-treated) adipocytes; $^{\#}$p < 0.05 *vs.* MaR1-treated brown adipocytes. ^{a}p < 0.05 *vs. Fgf21*$^{-/-}$ (vehicle-treated) brown adipocytes.

Member C (*Cd11c*), while the expression of anti-inflammatory genes (*Adipoq, Interleukin 10, Il10*) showed a similar induction to that observed in DIO mice. Interestingly, MaR1-treated mice also exhibited higher levels of *Interleukin 4* (*Il4*), an inducer of M2 macrophage polarization, and *Cluster of Differentiation 206* (*Cd206*), a M2 macrophage marker, as compared to control mice (Figure 2E). Immunofluorescence analyses revealed increased CD206 signals, a specific M2 macrophage marker, in iBAT of MaR1-treated mice (Figure 2F). Next, it was evaluated if treatment with MaR1 could improve the thermogenic response to cold exposure. Interestingly, when DIO mice treated with MaR1 were acutely (1 h) exposed to 4 °C, they lost more body weight (Figure 2G) and were able to better maintain rectal temperature, compared to vehicle-treated DIO mice (Figure 2H). Moreover, the microPET data revealed that MaR1-treated DIO mice exhibited higher ^{18}F-FDG uptake by iBAT (Figure 2I). Acute treatment with MaR1 also stimulates iBAT ^{18}F-FDG uptake and interscapular skin temperature assessed by infrared-thermography (Figure S1A-B). Taken together, all these observations strongly support MaR1 as a novel agent promoting iBAT activation in DIO mice.

MaR1 was also able to induce browning markers in iWAT of DIO mice, as revealed by the increase in UCP1 protein expression (Figure 3A), the up-regulation of genes related to mitochondrial biogenesis and mitochondrial fatty acid oxidation (Figure 3B). Additionally, iWAT from MaR1-treated mice exhibited increased expression levels of genes that typify beige adipocytes (*T-box 1 transcription factor*, *Tbx1*; *Transmembrane protein 26, Tmem26* and *Prdm16*), as well as of *Gpr120* and *Fgf21*, which have been also related with the browning process (Figure 3C). Again, this occurs in parallel with a reduction of inflammatory genes (*Tnfa, Ccl2*) and of M1 macrophages markers and an increase of M2 alternatively-activated macrophages (Figure 3D,E). Immune-adipose interactions may be key regulators to increase fat thermogenesis [45]. In fact, M1:M2 macrophages balance seems to play a role in iBAT activation and iWAT browning. Nguyen et al. [46] proposed that anti-inflammatory M2 macrophages are likely directly

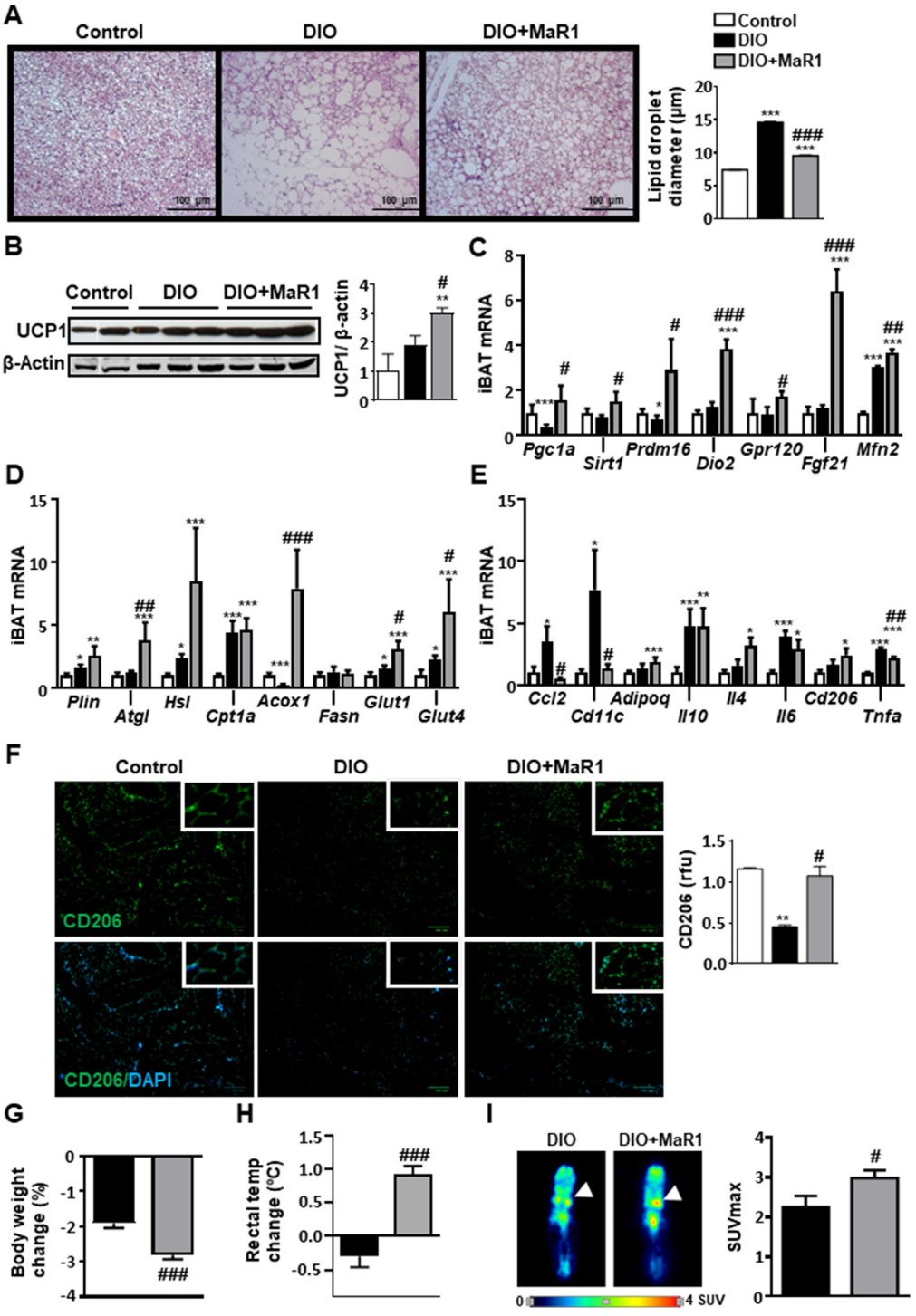

Figure 2: MaR1 promotes brown adipose tissue (BAT) activation in DIO mice. Twenty weeks-old DIO mice were daily treated either with MaR1 (50 µg/kg) or vehicle by oral gavage for 10 days. (A) Representative photomicrographs (magnification 100×) of iBAT sections stained with H&E dye (left panel) and lipid droplet size quantification (right panel) (n = 3). (B) Representative blot and densitometry analysis of iBAT UCP1 (band densities were normalized to β-Actin (n = 3–6). (C–E) mRNA expression levels of master mitochondrial biogenesis and function regulators and iBAT activator genes (C), and of genes involved in iBAT lipid metabolism and glucose uptake (D) as well as in inflammation and macrophage type markers (E) (n = 5–8). Data (mean ± SEM) are expressed as fold change relative to control (vehicle-treated) mice and considered as 1. (F) Representative images of IHF labelling of CD206 in iBAT (left), and quantification of immunoreactive signals (right panel) (n = 2). (G–H) Body weight changes and rectal temperature changes after acute (1 h) cold exposure (4 °C) in DIO mice treated with MaR1 (n = 5). (I) ^{18}F-FDG uptake using microPET 1 h after ^{18}F-FDG injection in mice pre-exposed for 1 h at 4 °C. Left panel: coronal sections of mice. White arrow: iBAT pads. Right panel: maximum standardized uptake value (SUVmax) (n = 3–5). Data (mean ± SEM). *p < 0.05; **p < 0.01; ***p < 0.001 vs. Control (vehicle-treated) mice; $^{\#}$p < 0.05; $^{\#\#}$p < 0.01; $^{\#\#\#}$p < 0.001 vs. DIO (vehicle-treated) mice.

involved in promoting BAT thermogenesis in mice. Moreover, IL-4 and adiponectin signaling have been reported to favour WAT beiging via cross-talk with resident macrophages by promoting M2 proliferation [45,47]. In our study, the activation of iBAT and beiging markers in MaR1-treated mice is also accompanied by an increase in *Il4*, *Adipoq* and M2 macrophages markers (Figure 3D,E), strongly suggesting that MaR1 could act in part through the regulation of M2 macrophages polarization in fat depots. Nevertheless, it is important to note that controversial observations about the direct role of alternatively activated macrophages in adaptive thermogenesis have been raised [48]. In order to get a better characterization of the role of macrophages on MaR1 actions on BAT, we cultured fully differentiated brown adipocytes with conditioned media of RAW 264.7 macrophages stimulated with LPS in the absence or presence of MaR1. Our data show that MaR1 (1 nM) reduced both basal and LPS-stimulated *Tnfa* mRNA expression in RAW 264.7 macrophages, suggesting that MaR1 is able to overcome the polarization to M1 macrophages induced by LPS (Figure S2A). Treatment of fully differentiated brown adipocytes with conditioned media from LPS-stimulated macrophages caused a significant downregulation of *Ucp1* mRNA expression, suggesting an impairment of thermogenic capacity. Interestingly, this inhibitory effect on *Ucp1* was not observed in brown adipocytes treated with conditioned media from LPS-stimulated macrophages co-treated with MaR1 (Figure S2B), suggesting that the crosstalk between macrophages and brown adipocytes could be also mediating the thermogenic effects of MaR1 observed in DIO-treated mice. Our current data suggest that iBAT activation and iWAT remodeling could contribute to the MaR1 moderate body fat lowering effects (Figures S3A-C) and to its previously reported insulin-sensitizing (Figure S3D) [19,49] and anti-steatotic properties in obese mice [50]. Although *Fgf2*1 mRNA levels were induced by MaR1 treatment in both iBAT and iWAT, we have previously reported that MaR1 downregulate hepatic *Fgf21* expression levels and decreases circulating FGF21 levels in DIO mice [20], suggesting that circulating FGF21 is not mediating the systemic thermogenic/metabolic actions of MaR1, in agreement with our observations in cultured brown adipocytes. It would have been of interest to determine if the current *in vivo* treatment with MaR1 (50 μg/kg, oral gavage, 10 days) could affect whole-body oxygen consumption, energy expenditure and physical activity in DIO mice, but unfortunately, we cannot provide these data. However, we characterized the effects of acute MaR1 administration (50 μg/kg, i. p., 24 h) in young (2-month-old) male mice fed on a normal chow diet. Our data show that acute treatment with MaR1 did not modify whole-body oxygen consumption or energy expenditure (Figures S4A-B). However, a significant increase in the respiratory exchange rate (RER) was observed in MaR1-treated mice, indicating that MaR1 promotes carbohydrate oxidation in mice fed with a high carbohydrate diet. Curiously, this increase in RER occurred only during the light period when MaR1 was administered (Figures S4C). This observation opens several questions: *i*) the relevance of carrying out MaR1 pharmacokinetic studies to determine the most effective dose and frequency of administration. Our observations suggest that it is probably necessary to administer MaR1 twice a day, just at the beginning and at the end of the light period in order to maintain the effect of MaR1 during the dark period, in which mice eat and are more active. *ii*) it would be of interest to characterize the effects on energy expenditure and RER in mice fed on a high fat diet to study if in this condition MaR1 is able to promote fat oxidation, and *iii*) to characterize if administration of MaR1 for a longer period could induce increased energy expenditure and weight loss.

On the other hand, our current data demonstrate the effectiveness of MaR1 to induce BAT activation after oral administration, a non-invasive and often safer route, which could be of relevance for its potential therapeutic use in obesity-related metabolic diseases. Indeed, targeted lipidomic analysis showed higher levels of MaR1 in BAT from MaR1-treated mice (Figure S5), suggesting that the induction of BAT activation observed in MaR1 could be partly mediated by a direct local action on this tissue; however, we cannot discard that other systemic actions could be also participating in this effect.

The fact that MaR1 can directly activate brown adipocytes in culture suggests that this SPM can also partly act in an adipocyte-autonomous manner. In line with this, we observed that the induction of the adipogenic process of hMSC, from subcutaneous WAT of obese subjects, in the presence of MaR1 increased the expression of several beige adipocyte-related genes including *UCP1*, *Cell death-inducing DFFA-like effector A* (*CIDEA*), *TMEM26*, *TBX1* [7], and also *PGC1α* (Figure 3F). This suggests that MaR1 could be effective in promoting the development of brite adipocytes in human WAT. The concentration of MaR1 necessary to induce browning of human white adipocytes is much higher than that required to activate murine brown adipocytes. Besides of species and adipocyte-type related differences, the need for a higher dose could be also due to the fact that the human adipocytes were obtained from obese subjects. Indeed, obesity reduced the browning capacity and also the physiological levels of SPMs in WAT and BAT in mice [24,51].

3.3. IL-6 is required for MaR1 effects on iBAT activation and iWAT browning

An interesting finding of our study was that MaR1 upregulates *Il6* mRNA levels both *in vitro* in cultured brown adipocytes (Figure 1A) and *in vivo* in iBAT of cold-exposed lean WT mice (Figure 4A). Several studies have related IL-6 and iBAT functions. Indeed, increased IL-6 expression was associated with thermogenic activation of brown adipocytes [52]. Moreover, the beneficial effects of iBAT transplantation on metabolic health were not observed in *Il6*-null mice [53]. A recent study has also shown that parabrachial IL-6 plays a key role in the regulation of iBAT thermogenesis and energy metabolism in mice [54]. Furthermore, IL-6 seems also to be required for the induction of WAT browning by cold exposure in mice [55].

Several of our current findings strongly support that the presence of IL-6 is required for the browning properties of MaR1: *i*) The stimulatory effects of MaR1 on thermogenic genes/proteins in *ex vivo* iBAT explants of WT mice were not observed in $Il6^{-/-}$ mice (Figure 4B). *ii*) The higher ^{18}F-FDG uptake by iBAT after cold exposure found in WT mice treated with MaR1 was not observed in *Il6* deficient mice (Figure 4C). *iii*) Non-invasively infrared-thermography revealed that the temperature of the interscapular skin laying directly above BAT was higher in MaR1-treated WT, but not in *Il6* deficient mice after short-term cold-exposure (Figure 4D). *iv*) The drop in rectal temperature induced by 24 h-cold exposure was prevented by MaR1 treatment in WT, but not in $Il6^{-/-}$ mice (Figure 4E). Moreover, the upregulation of thermogenic genes/proteins in iBAT (Figure 4F) and iWAT (Figure 4G) observed in WT mice treated with MaR1 was abrogated in $Il6^{-/-}$ mice treated with this SPM. *v*) Interestingly, the administration of recombinant IL-6 (rIL-6) to cold exposed *Il6*-deficient mice restored the stimulatory effect of MaR1 on thermogenic genes in iBAT and iWAT (Figure 4H,I). All these data strongly support that the presence of IL-6 is required for MaR1-thermogenic actions, at least after acute administration in cold-exposed lean mice. It is important to note that with our current data it cannot be established whether IL-6 plays a permissive or an active role on MaR1 thermogenic actions. IL-6 also mediates the metabolic benefits of protectin DX (PDX), another DHA-derived SPM. However, PDX insulin-sensitizing actions take place through a myokine-liver

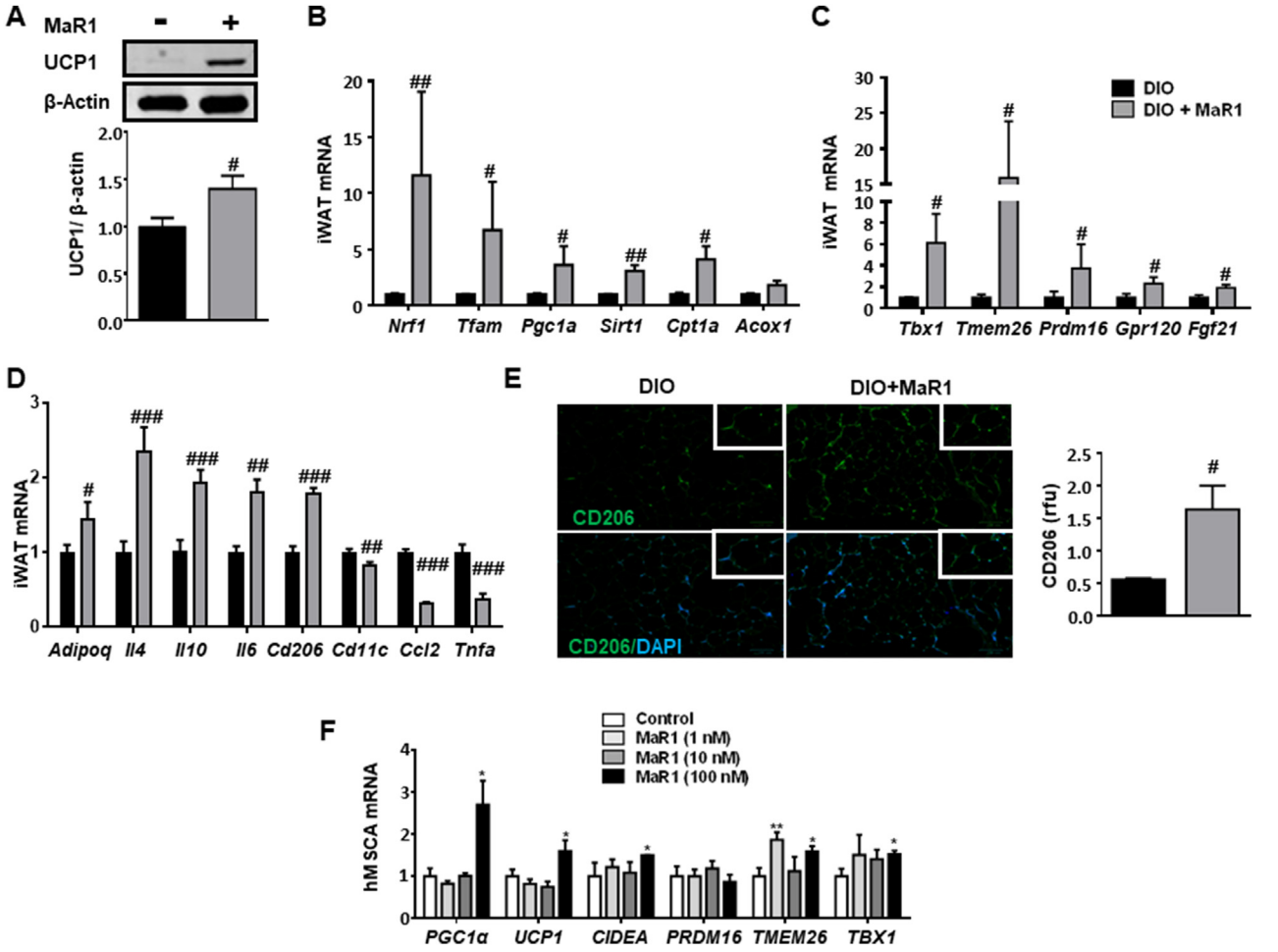

Figure 3: MaR1 induces beige adipocyte markers in iWAT of DIO mice and in human mesenchymal stem cells (hMSC)-derived adipocytes. (A–D) UCP1 protein (A), and mRNA expression levels of key regulators of mitochondrial biogenesis and fatty acid oxidation genes (B), and of beige/browning characteristic genes (C) as well as of genes related with inflammation and macrophage polarization (D) in iWAT from 20 weeks-old DIO mice treated with MaR1 (50 μg/kg) or vehicle by oral gavage for 10 days. Data (mean ± SEM) are expressed as fold change relative to DIO mice-treated with vehicle and considered as 1. ($n = 5–8$). $^{\#}p < 0.05$, $^{\#\#}p < 0.01$, $^{\#\#\#}p < 0.001$ *vs.* DIO mice. (E) Representative images of IHF labelling of CD206, and quantification of immunoreactive signals in iWAT of 20 weeks-old DIO mice treated with MaR1 (50 μg/kg) or vehicle by oral gavage for 10 days. ($n = 2–3$) $^{\#}p < 0.05$ *vs.* DIO mice. (F) mRNA expression levels of genes characteristics of the beiging process in hMSC treated along the differentiation process with MaR1 (1–100 nM). Determinations were carried out in fully differentiated hMSC-derived adipocytes. Data (mean ± SEM) are expressed as fold change relative to control cells, treated with vehicle and considered as 1. ($n = 2–5$). $^{*}p < 0.05$; $^{**}p < 0.01$ *vs.* vehicle-treated adipocytes.

glucoregulatory axis, and it seems to be independent of IL-6 activation in brown adipocytes in mice [56]. In contrast, MaR1 activates *Il6* expression mainly in iBAT (close 6-fold increase), and only a moderate upregulation was also found in muscle (around 1.5-fold increase), but not in epididymal WAT (eWAT) or liver of cold-exposed mice (see Figure S6A), suggesting that iBAT could be mainly contributing to the marginally higher levels of circulating IL-6 observed after acute treatment with MaR1 in these cold-exposed WT mice (Figure S6B). A limitation of our study is that we could not test the chronic actions of MaR1 (oral gavage) in diet-induced obese *Il6* deficient mice. Therefore, future studies should be performed to better characterize the role of IL-6 in the chronic actions of MaR1 on iBAT of DIO mice housed at room temperature or thermoneutrality.

3.4. LGR6 receptor mediates the MaR1-induced upregulation of thermogenic genes in fully differentiated murine brown adipocytes

Recently, Chiang et al. [57] identified Leucine Rich Repeat Containing G Protein-Coupled Receptor 6 (LGR6) as the receptor activated by MaR1, and mediating MaR1's proresolving functions in phagocytes. We found that *Lgr6* is also expressed in iBAT and iWAT, and its expression is upregulated after chronic treatment with MaR1 in DIO mice (Figure 5A). Similarly, *Lgr6* mRNA levels were also increased in cultured differentiated brown adipocytes treated with MaR1 (Figure 5B), further suggesting a potential role of the LGR6 receptor in MaR1 thermogenic actions. In order to elucidate the involvement of LGR6 activation in the thermogenic actions of MaR1, we evaluated the effect of MaR1 in LGR6-depleted brown adipocytes using siRNA (Figure 5C–E). Our data revealed that the MaR1-induced upregulation of *Ucp*1 and *Pgc1a* mRNA levels was abolished after silencing LGR6 expression in fully differentiated brown adipocytes (Figure 5D,E). These data suggest that LGR6 receptor is mediating the stimulatory effects of MaR1 on thermogenic regulators in cultured brown adipocytes. Future research should be performed to characterize if all the *in vivo* actions of MaR1 on brown/beige adipose tissue are also dependent of LGR6 receptor by analyzing the effects of MaR1 administration on adipose tissue-specific *Lgr6* knockout mice.

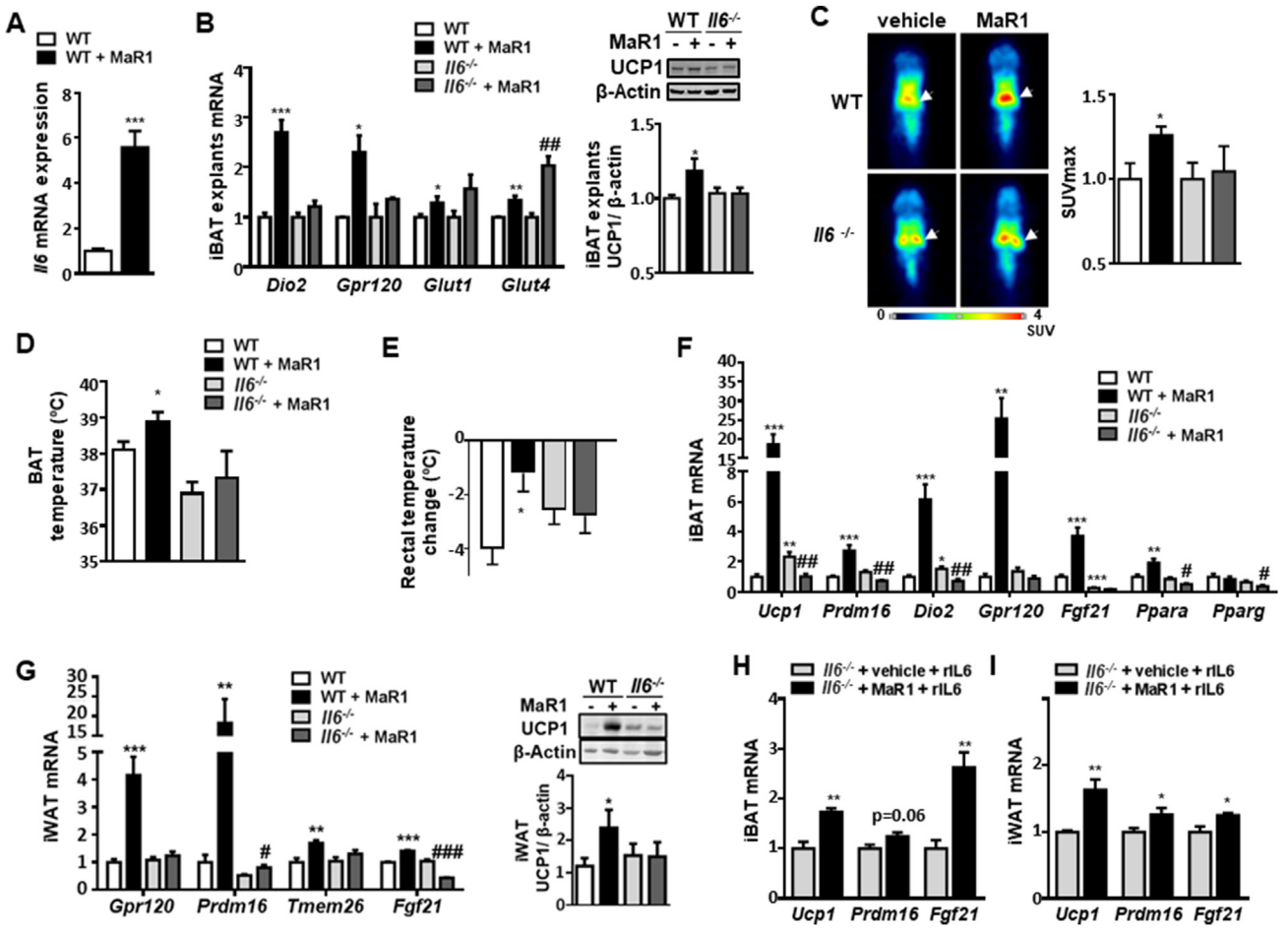

Figure 4: IL-6 is required for the stimulatory effect of MaR1 on BAT and WAT browning. (A) Acute MaR1 treatment (24 h, 50 μg/kg; i. p.) upregulates *Il6* mRNA levels in iBAT of cold-exposed (4 °C, 24 h) lean WT mice. Data are expressed as mean ± SEM (n = 7). ***p < 0.001 *vs.* WT (vehicle-treated) mice. (B) MaR1 (1 nM) stimulates thermogenic genes/proteins in *ex vivo* iBAT explants of lean WT, but not in $Il6^{-/-}$ mice. (n = 4–7). Data are expressed as fold change relative to WT mice-treated with vehicle and considered as 1. *p < 0.05; **p < 0.01; ***p < 0.001 *vs.* WT (vehicle-treated) mice; ##p < 0.01 *vs.* $Il6^{-/-}$ (vehicle-treated) mice. (C) BAT activity assessed by ^{18}F-FDG microPET in lean WT or $Il6^{-/-}$ mice treated with MaR1 (50 μg/kg; i. p.) or vehicle, and then exposed for 1 h at 4 °C, prior injection of ^{18}F-FDG. Left panel: coronal sections of mice. White arrow: iBAT pads. Right panel: maximum standardized uptake value (SUVmax). (n = 3–5). *p < 0.05 *vs.* WT (vehicle-treated) mice. (D) Temperature of the skin BAT area measured by infrared thermal images after 1 h cold exposure with or without MaR1 (50 μg/kg, i. p.) in lean WT or $Il6^{-/-}$ mice. (n = 4–9). *p < 0.05 *vs.* WT (vehicle-treated) mice. (E) Changes in rectal temperature in lean WT or $Il6^{-/-}$ mice treated (i.p.) with MaR1 (50 μg/kg) or vehicle and exposed for 24 h at 4 °C. (n = 6–7). *p < 0.05 *vs.* WT (vehicle-treated) mice. (F–G) Expression of thermogenic genes/proteins in iBAT (F) and iWAT (G) of lean WT or $Il6^{-/-}$ mice treated with MaR1 (50 μg/kg; i. p.) or vehicle and exposed for 24 h at 4 °C. (n = 3–7). *p < 0.05; **p < 0.01; ***p < 0.001 *vs.* WT (vehicle-treated) mice; #p < 0.05; ##p < 0.01; ###p < 0.001 *vs.* $Il6^{-/-}$ (vehicle-treated) mice. (H–I) Administration of recombinant IL-6 (rIL-6) (3.2 ng/kg, twice, every 12 h, i. p.) restores the stimulatory effect of MaR1 on thermogenic genes in iBAT (H) and iWAT (I) of lean $Il6^{-/-}$ mice exposed for 24 h at 4 °C. Data are expressed as fold change relative to $Il6^{-/-}$ mice treated with vehicle and rIL-6 and considered as 1. (n = 5). *p < 0.05, **p < 0.01 *vs.*$Il6^{-/-}$ (vehicle + rIL-6-treated) mice.

On the other hand, a study has revealed a key role of 12-LOX in BAT response to cold exposure, mainly by producing the lipid mediator 12-HETE [23]. 12-LOX is a key enzyme in MaR1 biosynthesis, and cold exposure also upregulates the expression of 14-HDHA, a precursor of MaR1, in iBAT and iWAT [23]. Moreover, cold exposure also upregulated EPHX1 and 2 in BAT of mice [11], which also participate in the biosynthesis of Maresins. In this way, our current studies have also found that cold exposure (4 °C, 24 h) increases the iBAT content of MaR1 and its precursor 14-HDHA, in parallel with the upregulation of the *Lgr6* mRNA expression as compared to room temperature-housed lean mice (Figure 6 A and B). All these findings and our current data suggest that increased MaR1 production and action could also be involved in physiological BAT activation by cold exposure. In our experimental conditions, we did not find any significant changes in MaR2 content in iBAT in response to cold exposure (data not shown). However, a recent study has revealed that a longer period of cold exposure (4 °C, 7 days) increased MaR2 and related structural isomers, but did not detect changes in MaR1 in BAT of high-fat diet fed obese mice as compared with those mice housed at thermoneutrality [58]. Although both studies are not comparable, they suggest differential *in vivo* effects of MaR1 and MaR2 administration on BAT and WAT. Thus, in contrast to what is observed in our current and previous studies with MaR1 [19], MaR2 treatment (10 μg/kg i. p., 26 days) did not significantly modulate expression of inflammatory genes in BAT or WAT [58]. In order to get a better insight on the potential differential effects of MaR2 and other SPMs in brown adipocytes, we treated fully differentiated murine brown adipocytes with MaR2, RvD1 and RvD2 (0.1–1 nM, 24 h). MaR2 exerted a moderate upregulation of *Ucp1* than MaR1, and in contrast to MaR1, it did not modify *Dio2* or even downregulated *Fgf2*1 mRNA (Figure S7A). RvD1 upregulated *Dio2*

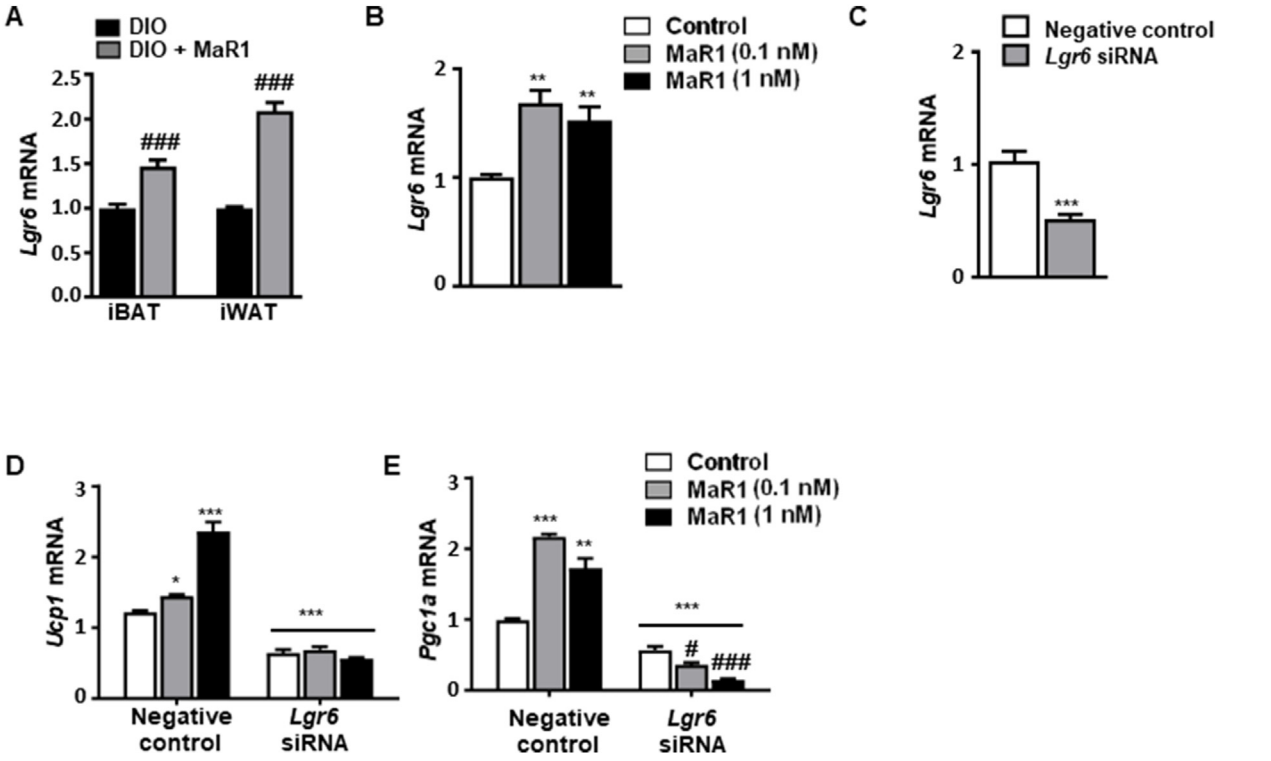

Figure 5: MaR1 promotes upregulation of thermogenic genes via LGR6 in fully differentiated murine brown adipocytes. (A–B) Expression of *Lgr6* in (A) iBAT and iWAT from 20 weeks-old DIO mice daily treated with MaR1 (50 μg/kg) or vehicle by oral gavage for 10 days (n = 5) and (B) mature brown adipocytes treated with vehicle or MaR1 (0.1, 1 nM) for 24 h (n = 4). $^{###}p < 0.001$ *vs.* DIO mice; $^{**}p < 0.01$ *vs.* control (vehicle-treated) brown adipocytes. (C) Reduced *Lgr6* mRNA levels in *Lgr6* siRNA-transfected brown adipocytes (n = 6). (D–E) *Ucp1* (D) and *Pgc1a* (E) mRNA levels in *Lgr6*-silenced brown adipocytes treated with vehicle or MaR1 (0.1, 1 nM) for 24 h (n = 5). Data are mean ± SEM. $^{*}p < 0.05$; $^{**}p < 0.01$; $^{***}p < 0.001$ *vs.* negative control siRNA brown adipocytes. $^{\#}p < 0.01$; $^{\#\#\#}p < 0.001$ *vs.* *Lgr6* siRNA brown adipocytes.

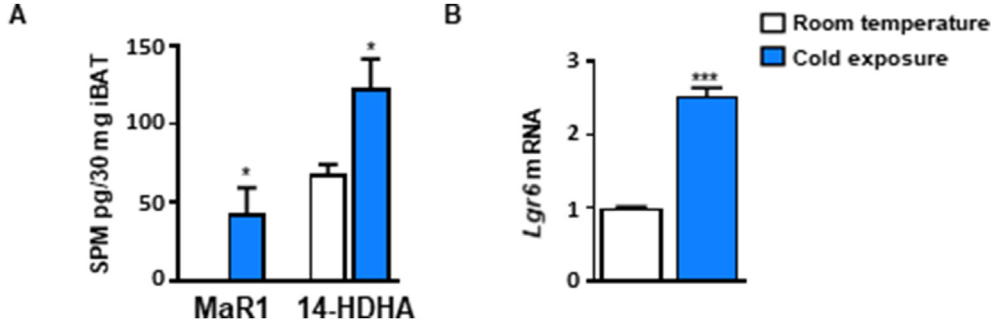

Figure 6: Cold exposure increases MaR1 and *Lgr6* levels in iBAT of lean mice. (A–B) Levels of MaR1 and 14-HDHA (A) and of *Lgr6* mRNA (B) in iBAT of sixteen-week-old male mice housed at room temperature or cold (4 °C) for 24 h. Data are mean ± SEM. (n = 3–6). $^{*}p < 0.05$; $^{***}p < 0.001$ *vs.* room temperature.

mRNA, no modified *Fgf21*, but at the dose of 1 nM downregulated *Ucp1* (Figure S7B). In contrast, RvD2 (1 nM) upregulated *Dio2, Fgf21* and *Ucp1* (Figure S7C). These data show differential metabolic effects of these SPMs on brown adipocytes, and suggest that MaR1 seems to be more effective in promoting brown adipocytes activation than the other DHA-derived SPMs tested. Interestingly, a previous study of our group found that the BAT of aged DIO mice have lower levels of SPMs than young mice, suggesting that the increase of inflammation and the drop of BAT activity that occurs during aging and obesity could be related to the decrease in Maresins and other SPMs [24]. These findings highlight the relevance of performing further studies to better understand the specific physiological/therapeutic actions on brown/beige adipose tissue of each SPMs. In summary, the current study provides first evidence of MaR1 acting as a novel inducer of iBAT activity and iWAT browning by regulating thermogenic program in adipocytes and polarization of M2 macrophages. Moreover, our data suggest that LGR6 receptor seems to mediate MaR1 actions on brown adipocytes, and that IL-6 is required for the thermogenic effects of MaR1. Furthermore, these thermogenic actions of MaR1 could contribute to its previously reported insulin sensitizing and anti-steatotic properties, representing a promising therapeutic agent to tackle obesity-associated metabolic disorders.

FUNDING

The authors received support for the current study from Ministerio de Ciencia e Innovación/Agencia Estatal de Investigación, Spain, MCIN/AEI/10.13039/501100011033 (grants BFU2012-36089 to MJM-A; BFU2015-65937-R to MJM-A, SL-C; PID2019-106982RB-I00 to MJM-A; SAF2017-83813-C3-1-R to LH and PID2021-122766OB-I00 to AMV), cofinanced by the European Regional Development Fund (ERDF); Dept. of Health, Navarra Government (67—2015) to MJM-A; Merck Health Foundation to LH; CIBEROBN (CB12/03/30002; CB06/03/0001; CB06/03/0025) and CIBERDEM (CB07/08/0033) from ISCIII (Spain). "Juan de la Cierva" Grant to MF-G (IJCI-2016-30025) funded by MCIN/AEI/10.13039/501100011033. Predoctoral grant to LML (Asociación de Amigos, Universidad de Navarra/"la Caixa" Banking Foundation) and to LM-F (FPI, BES-2013-064970). S.Q.-V. is supported by a fellowship from the Vicente Lopez Program (Eurecat).

AUTHOR'S CONTRIBUTIONS

MJM-A directed the research; XE, NS, MF-G, SL-C, FV collaborated in the experimental design. LML, XE, NS, IC-M and LM-F conducted the animal experiments; LML, NS, XE and EF-S performed mRNA expression and protein experiments; LML, XE and MF-G analyzed histological images; ES and CMR-O collaborated in Seahorse experiments; MC performed MicroPET scan studies; LML and NS performed experiments in the human mesenchymal stem cells and in brown adipocytes; AMV and JMA-M provided and collaborate in the *in vitro* studies with brown adipocytes and human mesenchymal stem cells, respectively; TQ-L, XE and FV participate in the studies in *Fgf21*$^{-/-}$ adipocytes. LH collaborated in the thermography studies; SQ-V and XE carried out the indirect calorimetry studies. JD performed the lipidomic analysis. MJM-A, XE, LML, NS and MF-G wrote the manuscript; and JAM, SL-C, CMR-O, ES, AMV, JMA-M, EF-S, LM-F, MC, TQ-L, IC-M, SQ-V, JD, LH and FV revised the manuscript.

DECLARATION OF COMPETING INTEREST

The authors declare that they have no known competing financial interests or personal relationships that could have appeared to influence the work reported in this paper.

DATA AVAILABILITY

Data will be made available on request.

ACKNOWLEDGEMENTS

We would like to thank Asunción Redín and Margarita Ecay for her valuable technical support on this project.

APPENDIX A. SUPPLEMENTARY DATA

Supplementary data to this article can be found online at https://doi.org/10.1016/j.molmet.2023.101749.

REFERENCES

[1] Yoneshiro T, Aita S, Matsushita M, Kayahara T, Kameya T, Kawai Y, et al. Recruited brown adipose tissue as an antiobesity agent in humans. J Clin Invest 2013;123:3404—8. https://doi.org/10.1172/JCI67803.

[2] Bartelt A, Bruns OT, Reimer R, Hohenberg H, Ittrich H, Peldschus K, et al. Brown adipose tissue activity controls triglyceride clearance. Nat Med 2011;17:200—5. https://doi.org/10.1038/nm.2297.

[3] Chondronikola M, Volpi E, Børsheim E, Porter C, Annamalai P, Enerbäck S, et al. Brown adipose tissue improves whole-body glucose homeostasis and insulin sensitivity in humans. Diabetes 2014;63:4089—99. https://doi.org/10.2337/db14-0746.

[4] Guerra C, Navarro P, Valverde AM, Arribas M, Brüning J, Kozak LP, et al. Brown adipose tissue—specific insulin receptor knockout shows diabetic phenotype without insulin resistance. J Clin Invest 2001;129:437. https://doi.org/10.1172/jci126191.

[5] Townsend KL, Tseng YH. Brown fat fuel utilization and thermogenesis. Trends Endocrinol Metabol 2014;25:168—77. https://doi.org/10.1016/j.tem.2013.12.004.

[6] Villarroya F, Cereijo R, Villarroya J, Giralt M. Brown adipose tissue as a secretory organ. Nat Rev Endocrinol 2017;13:26—35. https://doi.org/10.1038/nrendo.2016.136.

[7] Wu J, Bostrom P, Sparks LM, Ye L, Choi JH, Giang AH, et al. Beige adipocytes are a distinct type of thermogenic fat cell in mouse and human. Cell 2012;150:366—76. https://doi.org/10.1016/j.cell.2012.05.016.

[8] Jeremic N, Chaturvedi P, Tyagi SC. Browning of white fat: novel insight into factors, mechanisms, and therapeutics. J Cell Physiol 2017;232:61—8. https://doi.org/10.1002/jcp.25450.

[9] Villarroya F, Vidal-Puig A. Beyond the sympathetic tone: the new brown fat activators. Cell Metabol 2013;17:638—43. https://doi.org/10.1016/j.cmet.2013.02.020.

[10] Ghandour RA, Colson C, Giroud M, Maurer S, Rekima S, Ailhaud G, et al. Impact of dietary ω3 polyunsaturated fatty acid supplementation on brown and brite adipocyte function. J Lipid Res 2018;59:452—61. https://doi.org/10.1194/jlr.M081091.

[11] Lynes MD, Leiria LO, Lundh M, Bartelt A, Shamsi F, Huang TL, et al. The cold-induced lipokine 12,13-diHOME promotes fatty acid transport into brown adipose tissue. Nat Med 2017;23:631—7. https://doi.org/10.1038/nm.4297.

[12] Maurer SF, Dieckmann S, Kleigrewe K, Colson C, Amri EZ, Klingenspor M. Fatty acid metabolites as novel regulators of non-shivering thermogenesis. Handb Exp Pharmacol 2019;251:183—214.

[13] Quesada-López T, Cereijo R, Turatsinze JV, Planavila A, Cairó M, Gavaldà-Navarro A, et al. The lipid sensor GPR120 promotes brown fat activation and FGF21 release from adipocytes. Nat Commun 2016;7. https://doi.org/10.1038/ncomms13479.

[14] Spite M, Clària J, Serhan CN. Resolvins, specialized proresolving lipid mediators, and their potential roles in metabolic diseases. Cell Metabol 2014;19:21—36. https://doi.org/10.1016/j.cmet.2013.10.006.

[15] Serhan CN, Yang R, Martinod K, Kasuga K, Pillai PS, Porter TF, et al. Maresins: novel macrophage mediators with potent antiinflammatory and proresolving actions. J Exp Med 2009;206:15—23. https://doi.org/10.1084/jem.20081880.

[16] Han YH, Shin KO, Kim JY, Khadka DB, Kim HJ, Lee YM, et al. A maresin 1/RORα/12-lipoxygenase autoregulatory circuit prevents inflammation and progression of nonalcoholic steatohepatitis. J Clin Invest 2019;129:1684—98. https://doi.org/10.1172/JCI124219.

[17] Dalli J, Zhu M, Vlasenko NA, Deng B, Haeggström JZ, Petasis NA, et al. The novel 13S,14S-epoxy-maresin is converted by human macrophages to maresin 1 (MaR1), inhibits leukotriene A_4 hydrolase (LTA_4H), and shifts macrophage phenotype. Faseb J 2013;27:2573—83. https://doi.org/10.1096/fj.13-227728.

[18] Saínz N, Fernández-Galilea M, Costa AGV, Prieto-Hontoria PL, Barraco GM, Moreno-Aliaga MJ. N-3 polyunsaturated fatty acids regulate chemerin in cultured adipocytes: role of GPR120 and derived lipid mediators. Food Funct 2020;11:9057—66. https://doi.org/10.1039/d0fo01445a.

[19] Martínez-Fernández L, González-Muniesa P, Laiglesia LM, Sáinz N, Prieto-Hontoria PL, Escoté X, et al. Maresin 1 improves insulin sensitivity and

attenuates adipose tissue inflammation in ob/ob and diet-induced obese mice. Faseb J 2017;31:2135–45. https://doi.org/10.1096/fj.201600859R.

[20] Martínez-Fernández L, González-Muniesa P, Sáinz N, Laiglesia LM, Escoté X, Martínez JA, et al. Maresin 1 regulates hepatic FGF21 in diet-induced obese mice and in cultured Hepatocytes. Mol Nutr Food Res 2019;63:e1900358. https://doi.org/10.1002/mnfr.201900358.

[21] Laiglesia LM, Lorente-Cebrián S, López-Yoldi M, Lanas R, Sáinz N, Martínez JA, et al. Maresin 1 inhibits TNF-alpha-induced lipolysis and autophagy in 3T3-L1 adipocytes. J Cell Physiol 2018;233:2238–46. https://doi.org/10.1002/jcp.26096.

[22] Jung TW, Kim HC, El-Aty AMA, Jeong JH. Maresin 1 attenuates NAFLD by suppression of endoplasmic reticulum stress via AMPK-SERCA2b pathway. J Biol Chem 2018;293:3981–8. https://doi.org/10.1074/jbc.RA117.000885.

[23] Leiria LO, Wang CH, Lynes MD, Yang K, Shamsi F, Sato M, et al. 12-Lipoxygenase regulates cold adaptation and glucose metabolism by producing the Omega-3 lipid 12-HEPE from Brown fat. Cell Metabol 2019;30:768–783.e7. https://doi.org/10.1016/j.cmet.2019.07.001.

[24] Félix-Soriano E, Sáinz N, Gil-Iturbe E, Collantes M, Fernández-Galilea M, Castilla-Madrigal R, et al. Changes in brown adipose tissue lipid mediator signatures with aging, obesity, and DHA supplementation in female mice. Faseb J 2021;35:1–19. https://doi.org/10.1096/fj.202002531R.

[25] Zhu Z, Wu C, Cheng W, Xing H, Dang Y, Li F. Brown adipose tissue can be activated or inhibited within an hour before 18F-FDG injection: a preliminary study with MicroPET. J Biomed Biotechnol 2011;2011:159834. https://doi.org/10.1155/2011/159834.

[26] Cereijo R, Gavaldà-Navarro A, Cairó M, Quesada-López T, Villarroya J, Morón-Ros S, et al. CXCL14, a Brown adipokine that mediates Brown-Fat-to-Macrophage communication in thermogenic adaptation. Cell Metabol 2018;28:750–763.e6. https://doi.org/10.1016/j.cmet.2018.07.015.

[27] Weir JB. New methods for calculating metabolic rate with special reference to protein metabolism. J Physiol 1949;109(1–2):1–9. https://doi.org/10.1113/jphysiol.1949.sp004363.

[28] Ortega-Molina A, Efeyan A, Lopez-Guadamillas E, Muñoz-Martin M, Gómez-López G, Cañamero M, et al. Pten positively regulates brown adipose function, energy expenditure, and longevity. Cell Metabol 2012;15:382–94. https://doi.org/10.1016/j.cmet.2012.02.001.

[29] Boutant M, Joffraud M, Kulkarni SS, García-Casarrubios E, García-Roves PM, Ratajczak J, et al. SIRT1 enhances glucose tolerance by potentiating brown adipose tissue function. Mol Metabol 2015;4:118–31. https://doi.org/10.1016/j.molmet.2014.12.008.

[30] Beaudry JL, Kaur KD, Varin EM, Baggio LL, Cao X, Mulvihill EE, et al. The brown adipose tissue glucagon receptor is functional but not essential for control of energy homeostasis in mice. Mol Metabol 2019;22:37–48. https://doi.org/10.1016/j.molmet.2019.01.011.

[31] Stöckli J, Zadoorian A, Cooke KC, Deshpande V, Yau B, Herrmann G, et al. ABHD15 regulates adipose tissue lipolysis and hepatic lipid accumulation. Mol Metabol 2019;25:83–94. https://doi.org/10.1016/j.molmet.2019.05.002.

[32] Perez-Diaz S, Garcia-Rodriguez B, Gonzalez-Irazabal Y, Valero M, Lagos-Lizan J, Arbones-Mainar JM. Knockdown of {PTRF} ameliorates adipocyte differentiation and functionality of human mesenchymal stem cells. Am J Physiol Cell Physiol 2017;312:C83–91. https://doi.org/10.1152/ajpcell.00246.2016.

[33] Moreno-Aliaga MJ, Pérez-Echarri N, Marcos-Gómez B, Larequi E, Gil-Bea FJ, Viollet B, et al. Cardiotrophin-1 is a key regulator of glucose and lipid metabolism. Cell Metabol 2011;14:242–53. https://doi.org/10.1016/j.cmet.2011.05.013.

[34] Fernández-Galilea M, Pérez-Matute P, Prieto-Hontoria PL, Houssier M, Burrell MA, Langin D, et al. α-Lipoic acid treatment increases mitochondrial biogenesis and promotes beige adipose features in subcutaneous adipocytes from overweight/obese subjects. Biochim Biophys Acta 2015;1851:273–81. https://doi.org/10.1016/j.bbalip.2014.12.013.

[35] Gómez EA, Colas RA, Souza PR, Hands R, Lewis MJ, Bessant C, et al. Blood pro-resolving mediators are linked with synovial pathology and are predictive of DMARD responsiveness in rheumatoid arthritis. Nat Commun 2020;27(1):5420. https://doi.org/10.1038/s41467-020-19176-z. 11.

[36] Colas RA, Gómez EA, Dalli J. Methodologies and procedures employed in the identification and quantitation of lipid mediators via LC-MS/MS. Res Sq 2020:1–16. https://doi.org/10.21203/rs.3.pex-1147/v1.

[37] Pistorius K, Ly L, Souza PR, Gomez EA, Koenis DS, Rodriguez AR, et al. MCTR3 reprograms arthritic monocytes to upregulate Arginase-1 and exert pro-resolving and tissue-protective functions in experimental arthritis. EBioMedicine 2022;79:103974. https://doi.org/10.1016/j.ebiom.2022.103974.

[38] Livak KJ, Schmittgen TD. Analysis of relative gene expression data using real-time quantitative PCR and the 2(-Delta Delta C(T)) Method. Methods 2001;25(4):402–8.

[39] Boutant M, Kulkarni SS, Joffraud M, Ratajczak J, Valera-Alberni M, Combe R, et al. Mfn2 is critical for brown adipose tissue thermogenic function. EMBO J 2017;36(11):1543–58. https://doi.org/10.15252/embj.201694914.

[40] Mahdaviani K, Benador IY, Su S, Gharakhanian RA, Stiles L, Trudeau KM, et al. Mfn2 deletion in brown adipose tissue protects from insulin resistance and impairs thermogenesis. EMBO Rep 2017;18(7):1123–38. https://doi.org/10.15252/embr.201643827.

[41] Orava J, Nuutila P, Lidell ME, Oikonen V, Noponen T, Viljanen T, et al. Different metabolic responses of human brown adipose tissue to activation by cold and insulin. Cell Metabol 2011;14:272–9. https://doi.org/10.1016/j.cmet.2011.06.012.

[42] Hondares E, Iglesias R, Giralt A, Gonzalez FJ, Giralt M, Mampel T, et al. Thermogenic activation induces {FGF}21 expression and release in brown adipose tissue. J Biol Chem 2011;286:12983–90. https://doi.org/10.1074/jbc.M110.215889.

[43] Villarroya F, Cereijo R, Villarroya J, Gavaldà-Navarro A, Giralt M. Toward an understanding of how immune cells control Brown and beige adipobiology. Cell Metabol 2018;27:954–61. https://doi.org/10.1016/j.cmet.2018.04.006.

[44] Alcalá M, Calderon-Dominguez M, Bustos E, Ramos P, Casals N, Serra D, et al. Increased inflammation, oxidative stress and mitochondrial respiration in brown adipose tissue from obese mice. Sci Rep 2017;7:1–12. https://doi.org/10.1038/s41598-017-16463-6.

[45] Qiu Y, Nguyen KD, Odegaard JI, Cui X, Tian X, Locksley RM, et al. Eosinophils and type 2 cytokine signaling in macrophages orchestrate development of functional beige fat. Cell 2014;157:1292–308. https://doi.org/10.1016/j.cell.2014.03.066.

[46] Nguyen KD, Qiu Y, Cui X, Goh YPS, Mwangi J, David T, et al. Alternatively activated macrophages produce catecholamines to sustain adaptive thermogenesis. Nature 2011;480:104–8. https://doi.org/10.1038/nature10653.

[47] Hui X, Gu P, Zhang J, Nie T, Pan Y, Wu D, et al. Adiponectin enhances cold-induced browning of subcutaneous adipose tissue via promoting M2 macrophage proliferation. Cell Metabol 2015;22:279–90. https://doi.org/10.1016/j.cmet.2015.06.004.

[48] Fischer K, Ruiz HH, Jhun K, Finan B, Oberlin DJ, Van Der Heide V, et al. Alternatively activated macrophages do not synthesize catecholamines or contribute to adipose tissue adaptive thermogenesis. Nat Med 2017;23:623–30. https://doi.org/10.1038/nm.4316.

[49] Martínez-Fernández L, González-Muniesa P, Sáinz N, Escoté X, Martínez JA, Arbones-Mainar JM, et al. Maresin 1 regulates insulin signaling in human adipocytes as well as in adipose tissue and muscle of lean and obese mice. J Physiol Biochem 2021;77:167–73. https://doi.org/10.1007/s13105-020-00775-9.

[50] Laiglesia LM, Lorente-Cebrián S, Martínez-Fernández L, Sáinz N, Prieto-Hontoria PL, Burrell MA, et al. Maresin 1 mitigates liver steatosis in ob/ob and

diet-induced obese mice. Int J Obes 2018;42:572—9. https://doi.org/10.1038/ijo.2017.226.

[51] Neuhofer A, Zeyda M, Mascher D, Itariu BK, Murano I, Leitner L, et al. Impaired local production of proresolving lipid mediators in obesity and 17-HDHA as a potential treatment for obesity-associated inflammation. Diabetes 2013;62:1945. https://doi.org/10.2337/db12-0828. —56.

[52] Burýšek L, Houštěk J. β-Adrenergic stimulation of interleukin-1α and interleukin-6 expression in mouse brown adipocytes. FEBS Lett 1997;411:83—6. https://doi.org/10.1016/S0014-5793(97)00671-6.

[53] Stanford KI, Middelbeek RJW, Townsend KL, An D, Nygaard EB, Hitchcox KM, et al. Brown adipose tissue regulates glucose homeostasis and insulin sensitivity. J Clin Invest 2013;123:215—23. https://doi.org/10.1172/JCI62308.

[54] Mishra D, Richard JE, Maric I, Porteiro B, Häring M, Kooijman S, et al. Parabrachial interleukin-6 reduces body weight and food intake and increases thermogenesis to regulate energy metabolism. Cell Rep 2019;26:3011—3026.e5. https://doi.org/10.1016/j.celrep.2019.02.044.

[55] Knudsen JG, Murholm M, Carey AL, Biensø RS, Basse AL, Allen TL, et al. Role of IL-6 in exercise training- and cold-induced UCP1 expression in subcutaneous white adipose tissue. PLoS One 2014;9:1—8. https://doi.org/10.1371/journal.pone.0084910.

[56] White PJ, St-Pierre P, Charbonneau A, Mitchell PL, St-Amand E, Marcotte B, et al. Protectin {DX} alleviates insulin resistance by activating a myokine-liver glucoregulatory axis. Nat Med 2014;20:664—9. https://doi.org/10.1038/nm.3549.

[57] Chiang N, Libreros S, Norris PC, De La Rosa X, Serhan CN. Maresin 1 activates LGR6 receptor promoting phagocyte immunoresolvent functions. J Clin Invest 2019;129:5294—311. https://doi.org/10.1172/JCI129448.

[58] Sugimoto S, Mena HA, Sansbury BE, Kobayashi S, Tsuji T, Wang CH, et al. Brown adipose tissue-derived MaR2 contributes to cold-induced resolution of inflammation. Nat Metab 2022;4(6):775—90. https://doi.org/10.1038/s42255-022-00590-0.

